

Pool Boiling Experiments on a Nano-Structured Surface

Hee Seok Ahn, Vijaykumar Sathyamurthi, and Debjyoti Banerjee

Abstract—The effect of nano-structured surfaces on pool boiling was investigated. Saturated and subcooled pool boiling experiments were performed on a horizontal heater surface coated with vertically aligned multiwalled carbon nanotubes (MWCNTs). MWCNTs were synthesized using the chemical vapor deposition (CVD) process. In this paper, MWCNT forests of two distinctly different heights (Type A: 9- μm height, and Type B: 25- μm height) were synthesized separately on silicon wafers. PF-5060 was used as the test liquid. The results show that Type-B MWCNTs yield distinctly higher heat fluxes under subcooled and saturated conditions for both nucleate and film boiling. Type-A MWCNTs provide similar enhancement in nucleate boiling (as Type-B) for both saturated and subcooled conditions. Type-B MWCNTs enhanced critical heat flux (CHF) by 40%. Increasing the height of the MWCNTs is also found to extend the wall super heat required for CHF. In contrast, Type-A MWCNTs provide only marginal enhancement in film boiling compared to bare silicon wafer, for both saturated and subcooled film boiling. Type-B MWCNTs enhanced the heat flux in the film boiling regime for the Leidenfrost point by 175% (compared to bare silicon wafer).

Index Terms—Carbon nanotube, cooling, critical heat flux (CHF), film boiling, Leidenfrost point, multiwalled, nucleate boiling.

I. INTRODUCTION

BOILING is the most efficient heat transfer mechanism. Hence, boiling is an attractive option for tackling the thermal management issues, particularly for the cooling of microprocessors and high heat flux electronic devices. Passive schemes for enhancing boiling heat transfer include: increased liquid subcooling, addition of surfactants and use of various types of engineered microstructured surface morphologies (e.g., surface micromachined structures, graphite foams, porous surfaces, etc.). Surface morphology and thermophysical properties of the heater surface are known to significantly modify the transport mechanisms during boiling heat transfer [1].

Many researchers reported the enhancement of heat transfer by using newly developed materials or structures combined with pool boiling. Ramaswamy *et al.* [2] conducted experiments

to investigate the combined effect of pressure and subcooling on boiling performance of enhanced structures. The enhanced structures were made of six layers of copper plates in which rectangular channels were cut on either side of plates. The combined effects of subcooling and pressure were found to enhance pool boiling heat transfer on these structures. Ramaswamy *et al.* [3] also performed experiments to investigate the effect of the dimensions of the enhanced structure on boiling performance. The authors parametrically changed the pore size, pitch, and height to optimize the dimensions for maximizing heat transfer. They postulated that the increase in pore size and reduction in pitch augmented the heat dissipation at low to intermediate wall super heat (4–12 K). Mudawar and Anderson [4] performed saturated as well as subcooled pool-boiling experiments using multilevels of low profile surfaces (microfins, microgrooves, and microstuds) and reported that the critical heat flux (“CHF”) of 159.3 W/cm² could be achieved at wall super heat of 65 °C and liquid subcooling of 35 °C using FC-72 as a working fluid. Coursey *et al.* [5] explored the applicability of graphite foams to thermal management of electronic devices. The foams are composed of graphite ligaments which are reported to have thermal conductivity values (up to five times higher than for copper). The bulk graphite foam are also reported to have thermal diffusivity values (up to four times higher than that of aluminum) due to the high thermal conductivity and low density. The effects of chamber pressure, liquid level, and working fluid on the nucleate boiling were considered in the experiments.

Using hexagonal dimples and trenches microfabricated on silicon wafers (~ 3 – $50 \mu\text{m}$ deep, ~ 11 – $12 \mu\text{m}$ -wide square patterns, ~ 22 – $110 \mu\text{m}$ pitch), Gebhart and Wright [6] reported pool boiling enhancement by 420% for saturated water. Miller *et al.* [7] used a similar experimental configuration using dimple structures (9.4- μm diameter, 3.3- μm depth, $\sim 15 \mu\text{m}$ pitch) on the surface of a silicon wafer to study the effect of microstructures on boiling incipience for saturated FC-72. Honda *et al.* [8] studied the effects of micropin fins and submicrometer-scale roughness on pool boiling heat transfer enhancement from a silicon surfaces using FC-72. Engineered submicrometer-scale roughness ($\sim 30 \text{ nm}$) was introduced on some of the surfaces. The maximum heat flux reported in this study was $\sim 60 \text{ W/cm}^2$ at a wall superheat of 35 °C and liquid subcooling of 45 °C. Larger heat transfer enhancement was observed on surfaces with submicrometer-scale roughness and the micro-pin fins were reported to augment heat transfer and CHF (1.8–2.3 times) compared to the plain surfaces. Analytical investigation by Bahrami *et al.* [9] showed that the random submicrometer-scale roughness distribution causes both cross-sectional area as well as surface area of the micropin

Manuscript received February 01, 2006; revised January 30, 2007 and October 09, 2007. Current version published February 27, 2009. This work was supported in part by the “New Investigator Program” of the Texas Space Grants Consortium, Texas Engineering Experimentation Station (TEES) and the Mechanical Engineering Department, Texas A&M University. This work was recommended for publication by Associate Editor S. Bhavani upon evaluation of the reviewers comments.

The authors are with the Mechanical Engineering Department, Texas A&M University, College Station, Texas 77843 USA (e-mail: aheeseok@tamu.edu; dbanerjee@tamu.edu).

Color versions of one or more of the figures in this paper are available online at <http://ieeexplore.ieee.org>.

Digital Object Identifier 10.1109/TCAPT.2009.2013980

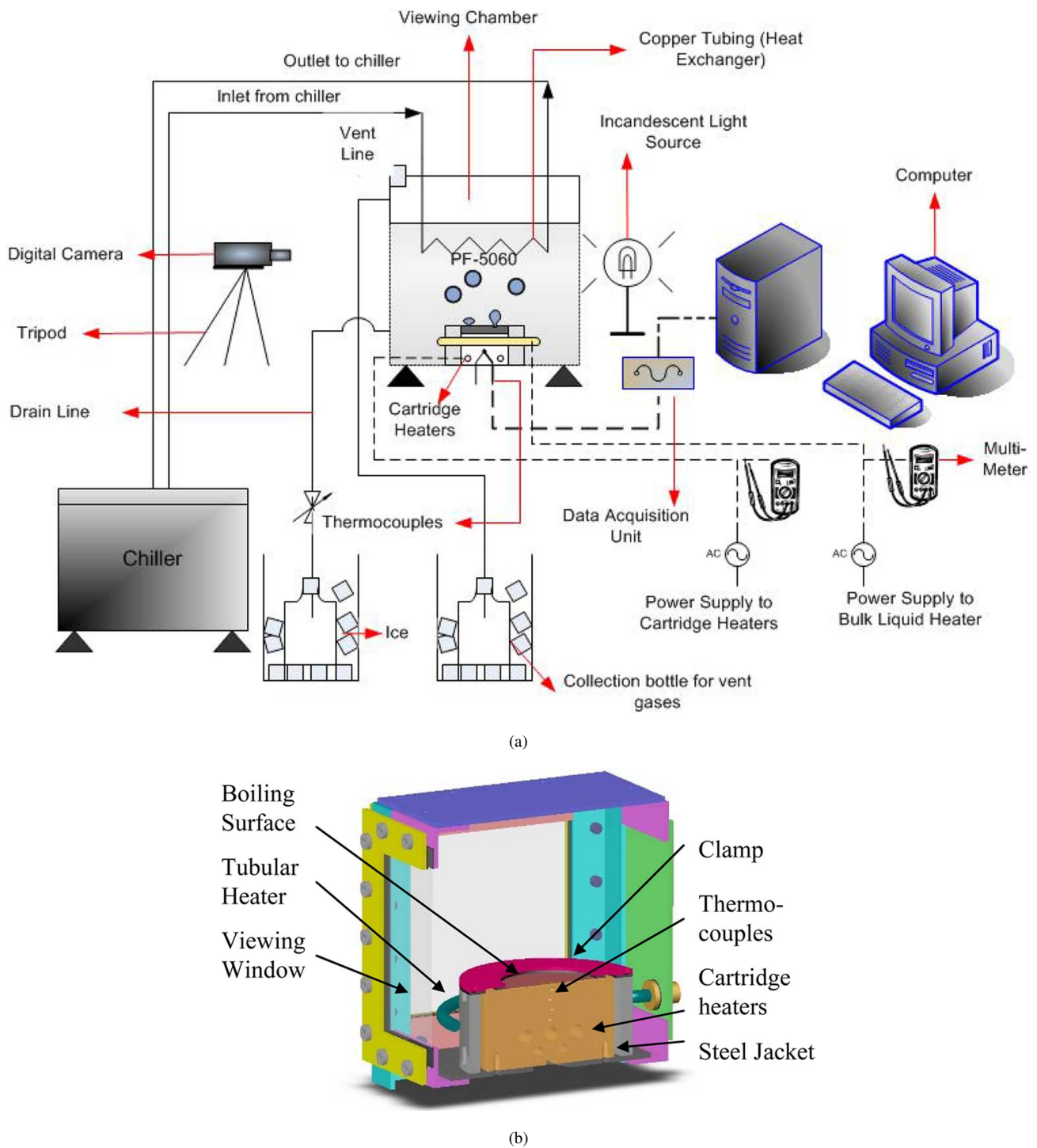


Fig. 1. (a) Schematic diagram of experimental apparatus. (b) Cross section of the viewing chamber.

fins to increase, resulting in heat transfer augmentation. This shows that nanoscale surface features can affect boiling heat transfer mechanism [10].

After discovery of carbon nanotubes (CNTs) by Iijama [11], various potential applications of CNTs have been envisioned. CNTs are particularly attractive materials due to their broad range of thermal, electrical, and structural properties that can be tailored to various molecular structural types (length, diameter, and orientation). According to Berber *et al.* [12], the

thermal conductivity value of single-walled CNT (SWCNT) is 6600 W/m-K (around 17 times higher than that of copper) at room temperature and drops drastically to 3000 W/m-K (around eight times higher than that of copper) at 400 K. The axial thermal conductivity of individual multiwalled CNT (MWCNT) was measured to exceed 3000 W/m-K by Kim *et al.* [13].

Ujereh *et al.* [14] reported pool boiling experiments using randomly oriented MWCNT arrays on a silicon surface. The experiments were performed for saturated pool boiling of

FC-72 on a horizontal heater under saturated conditions. The heater area was $12.7 \text{ mm} \times 12.7 \text{ mm}$. The MWCNT were synthesized by using a calcined dendrimer precursor for the plasma enhanced chemical vapor deposition process (PECVD). The MWCNTs were 30 nm in diameter and 20–30 μm in length. Heat transfer enhancement of 60% was obtained for a critical heat flux (CHF) of 15 W/cm^2 . The experimental error in the data was not reported. The study was restricted to nucleate boiling conditions and the performance of the nano-structured surface under film boiling conditions was not reported. Also, the authors noted that the synthesized MWCNTs did not provide complete surface coverage. The authors reported that significant degradation of the MWCNT structures was not observed at the end of the experiment—showing good bonding of the MWCNT to the substrate.

This paper is an extension of the saturated pool boiling studies by Ahn *et al.* [15]. In this paper, heat flux values are compared from experiments for both saturated and subcooled conditions during pool boiling for both nucleate and film boiling on a bare silicon wafer and two silicon wafers, each coated with MWCNTs of a different height (9 and 25 μm). The working fluid used in this experiment was PF-5060 (Manufacturer: 3M Co.). PF-5060 (which is 95% pure FC-72 [5]) was chosen as the working liquid as a cheaper substitute for FC-72. Both liquids have nearly identical boiling characteristics (e.g., latent heat of vaporization, saturation temperature, liquid and vapor densities as well as specific heats, etc.). For this purpose, an experimental apparatus was built that consisted of a viewing chamber housing a silicon wafer coated with MWCNTs (which was clamped on top of a heater apparatus) and a heat exchanger apparatus connected to a chiller unit. Scanning electron microscope (SEM) images of the MWCNT-coated surfaces were obtained before and after the experiments to verify any change in the inherent morphology. Also, uniform surface coverage of MWCNTs on the silicon wafer substrate was obtained during the synthesis using the chemical vapor deposition (CVD) process.

The presence of grooves and pits on commercial surfaces are known to alter the nucleation site density on a boiling surface [1]. Hence, to gauge the heat transfer augmentation purely due to the presence of the MWCNTs, an atomically smooth bare silicon wafer was chosen as the substrate for the experiments used in this study. In the absence of nucleation cavities on the pool boiling surface, the heat flux obtained in this paper is much lower than for commercial surfaces (e.g., on a copper heater). However, the primary motivation of this study was to investigate how the nano-structured surfaces perturb the various transport mechanisms for the different pool boiling regimes. Such insights gathered from this study can therefore help in designing and developing enhanced heat transfer surfaces specifically tailored for electronics chip cooling applications using pool boiling.

II. EXPERIMENTAL APPARATUS

The experimental apparatus used in this study consisted of 1) a viewing chamber, which is used to house 2) a heater apparatus (consisting of copper block covered with a steel jacket and embedded thermocouples and cartridge heaters), with 3) a

silicon wafer mounted on top and 4) a heat exchanger apparatus for liquid subcooling (consisting of a chiller and coiled copper tubing). The temperature measurements were recorded using a computer-controlled high speed data acquisition system. Fig. 1 shows the schematic diagram of the experimental setup and the cross section of the viewing chamber.

A. Test Apparatus

A heater apparatus was placed inside the viewing chamber [Fig. 1(b)]. The heater apparatus consists of a cylindrical copper block (8.89 cm in diameter) which was enclosed by an annular steel jacket. A silicon wafer was placed on top of the copper block and clamped with an annular steel disk. A Pyrex wafer was placed between the silicon wafer and the copper block to minimize the electrical noise from heaters. Holes were drilled on the top and bottom of the steel jacket and threads were formed in the holes using a tap. Bolts were screwed into the holes to clamp the steel disk on the silicon wafer. Five holes were drilled into the side of the cylindrical copper block for placing cartridge heaters (three of 500-W rating and two of 300-W rating, manufactured by Watlow, Inc.). Twelve holes were drilled at different depths and radial locations along the side of the copper block, and K-type thermocouples were placed in these holes for measuring the temperature distribution in the copper block. K-type thermocouples were placed along the sides of the frame to measure the temperatures and estimate the heat loss to the surrounding.

One thermocouple was placed in the liquid PF-5060 to measure the bulk liquid temperature. Some of the experiments were subsequently repeated with three thermocouples for measuring the bulk liquid temperatures for the same wall superheat and liquid subcooling. It was observed from the experiments using three thermocouples that the bulk liquid temperature was fairly uniform (within $\pm 0.5 \text{ }^\circ\text{C}$ for saturated experiments and within $\pm 1 \text{ }^\circ\text{C}$ for subcooling of up to $10 \text{ }^\circ\text{C}$) due to the vigorous mixing within the bulk liquid pool caused by bubble motion during pool boiling.

B. Viewing Chamber

The viewing chamber was constructed for performing pool boiling experiments and is shown in Fig. 1(b). Mild steel L-Beams (0.32 cm thick and 2.54 cm wide) were used to form the structural frame of the chamber. The beams were cut and welded together to form a cubic chamber, having a side length of 15.24 cm. A steel base plate was placed at the top and bottom of the chamber. Pyrex glass sheets (0.32 cm thick) were mounted on three sides of the chamber. To prevent cracking due to differential thermal expansion, the glass sheets were backed by rubber gaskets on either side and clamped with steel square frames which were machined to appropriate size. The glass and the steel plate were mounted using nuts, bolts, and washers [Fig. 1(b)]. Several holes were drilled into the steel plate for mounting the tubular heaters and for venting the chamber. The vent was made to prevent the pressure in the viewing chamber from rising above atmospheric pressure. The vent was connected to an open chamber using a copper tube. The chamber was dipped in ice water for condensing and reclaiming the vaporized PF-5060.

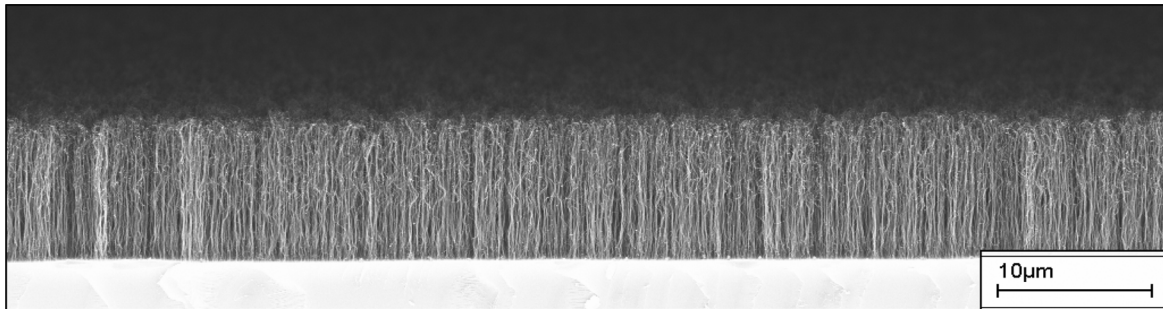


Fig. 2. SEM image of MWCNTs synthesized on silicon wafer.

C. Chiller Apparatus for Subcooled Experiments

For subcooled boiling experiments, a coiled copper tube was dipped just below the surface of the test fluid of PF-5060 to keep the test fluid at a constant temperature to achieve subcooling of 5 °C and 10 °C [Fig. 1(a)]. The coiled copper tube was connected to a constant temperature refrigerating/heating circulator bath (manufacturer: PolyScience, Model 9612) containing antifreeze (50% ethylene glycol solution in water). The antifreeze solution was pumped and recirculated in the copper tube from the constant temperature bath. The flow rate and the temperature of the glycol solution in the copper tube were controlled to achieve the desired subcooling of PF-5060 during the experiments. To minimize the heat loss from the working fluid to the environment, an insulation tape was wrapped around the copper tubing connectors between the test section and the constant temperature bath. During the saturated boiling experiments, the coiled copper tubing was lifted above the surface.

D. Synthesis of MWCNTs on Silicon Wafer

MWCNT forests were grown on the silicon wafer using CVD techniques. The MWCNT structures (“forests”) obtained by CVD were uniform in height. Two different wafers coated with two different heights of MWCNT forests were used in the experiments (Type-A: 9 μm and Type-B: 25 μm height). Fig. 2 shows the SEM images of the silicon wafer substrates containing MWCNT forests. Details about the CVD process for synthesis and growth of MWCNT forests are described in [16]. Typically, 8–15 nm diameter vertically aligned MWCNT “forests” are synthesized by flowing 5 mol% C_2H_2 at 580 sccm in He using the CVD process at atmospheric pressure in a quartz tube furnace maintained at 680 °C. The synthesis time can range from a few seconds to ~ 20 min since the growth rates of the MWCNTs are $\sim 1\text{--}2$ $\mu\text{m}/\text{minute}$. An iron film of 5-nm thickness was deposited by electron beam evaporation to serve as a catalyst. Earlier investigations [16] using SEM and thermal gravimetric measurements indicated that the purity of the synthesis process was very high ($\sim 96\text{--}98\%$ carbon in the form of MWCNTs) with 2%–4% Fe and amorphous carbon (no carbon particles were observed in this investigation).

III. EXPERIMENTAL PROCEDURE

Pool boiling experiments were conducted under steady-state conditions. The heat input to the test section was varied by changing the voltage supply to the heaters which was adjusted by a variac. For nucleate boiling experiments, the voltage input

were increased in increments of 1–5 V, starting from a base value of 16 V until the CHF point was reached. To obtain CHF data, the voltage input to the heaters was reduced promptly just before an abrupt temperature increment was detected, followed by small incremental adjustment of the voltage values to achieve the maximum heat flux value. After obtaining the steady-state data at maximum heat flux value (CHF), the voltage input was slightly increased to force transition into film boiling. This was followed by rapidly decreasing the heat input to the test section and setting the variac to a smaller input voltage. This was used to obtain steady-state film boiling. For the film boiling experiments the input voltage was gradually reduced by successive decrements in the range of 0.5–2 V before the regime changed from film to nucleate boiling. This procedure was used to estimate the “hysteresis” in the boiling curve. Typically, each voltage setting required 2–3 h for achieving steady-state temperature conditions for both nucleate and film boiling. Longer time was required to achieve steady-state conditions in film boiling. Typically, boiling experiments for saturated conditions were performed continuously for 24–36 h and the experiments for subcooled conditions were performed continuously for 36–40 h to obtain all the data points reported in this study for each substrate (bare silicon wafer and Type-A and Type B MWCNTs).

For the experiments under the subcooled conditions, the heat exchanger tubes were lowered to the level of around 1.5 cm below from the free surface of the liquid in the chamber, and the temperature of the cooling unit was adjusted manually to achieve the desired degree of subcooling temperature. For all experiments, the liquid level was fixed at 5 cm above the heated surface, and the working liquid was added (replenished) periodically in the test section to maintain the liquid level constant. The liquid replenishment was performed prior to establishing steady-state temperature conditions.

After steady-state conditions were reached, the temperature data from the thermocouples were recorded with a computer-controlled data acquisition system. The data acquisition system consisted of NI SCXI-1102C Analog MUX, and PCI-6251 DAQ Board with Pentium 4 3.2-GHz computer, and controlled by a program using Labview 7.1 software. Sampling rate for measuring the temperature variation was 200 Hz. To estimate the power input to the test section during the experiment, the voltage and current inputs were measured with a digital TRMS voltmeter and a clamp ammeter, respectively.

The heat flux was evaluated from the gradient of the temperature profiles in the copper block. The wall temperature

values of the silicon wafer were estimated by utilizing thermal resistance values obtained from prior temperature measurements using surface micromachined thin film thermocouple (TFT) on the silicon wafer [17]. The total uncertainty of the temperature differential was estimated to be ± 0.055 °C. The estimated uncertainty in temperature measurement was $\pm 6.6\%$ and $\pm 16.3\%$ at CHF and Leidenfrost points, respectively. Using uncertainty values of $\pm 1.0\%$ for thermal conductivity of copper block and of $\pm 3.0\%$ for the vertical distance between two thermocouples embedded in the copper block, the estimated uncertainty values of the heat flux are $\pm 7.3\%$ at CHF point (wall super heat = 69 °C under 5 °C subcooled condition for bare silicon wafer) and $\pm 24.3\%$ at Leidenfrost point (wall super heat = 60 °C under saturated condition for bare silicon wafer).

IV. EXPERIMENTAL RESULTS

Saturated and subcooled experiments were performed to study the effect of liquid subcooling on the efficacy of the nano-structured surfaces in enhancing heat transfer. The heat transfer enhancement obtained by using the nano-structured surfaces was compared to the heat transfer data obtained from a smooth surface using a smooth bare silicon wafer (this served as the control experiment). As mentioned before, the presence of grooves and pits on commercial surfaces are known to alter the nucleation site density on a boiling surface [1]. Hence, to gauge the heat transfer augmentation purely due to the presence of the MWCNT, an atomically smooth bare silicon wafer was chosen for the control experiments.

A. Control Experiments on Bare Silicon Wafer

In Fig. 3, hollow markers represent pool boiling data for PF-5060 on bare silicon wafer under saturated and subcooled (5 °C and 10 °C) conditions. In the nucleate boiling regime, the pool boiling heat flux was higher for subcooled liquid than for saturated liquid. Pool boiling heat flux was enhanced significantly at CHF as the liquid subcooling was increased. The CHF condition was obtained at wall super heat of 87 °C and the associated heat flux was 4.8×10^4 W/m² under 10 °C subcooled conditions. Inception of film boiling was obtained by decreasing the power input to the heaters just after rapid increase in wall temperature was detected from the data acquisition system beyond the CHF point. Since steady-state conditions were difficult to obtain at the Leidenfrost point (“minimum heat flux” in film boiling), the experimental data were recorded close to the Leidenfrost point. The heat flux at Leidenfrost point was observed to be 8.6 kW/m² for saturated liquid and was found to increase marginally with subcooling to a value of 1.3×10^4 W/m² for liquid subcooling of 10 °C. From the experimental results, Leidenfrost point appeared at increasingly higher wall superheat as the degree of subcooling was increased. Leidenfrost point was obtained at 74 °C, 70 °C, and 60 °C for liquid subcooling of 10 °C, 5 °C and saturated conditions, respectively.

B. Experiments Using Type-A MWCNT Forests

Experiments were conducted for silicon wafer coated with Type-A MWCNT (9- μ m height). In Fig. 3, solid markers depict

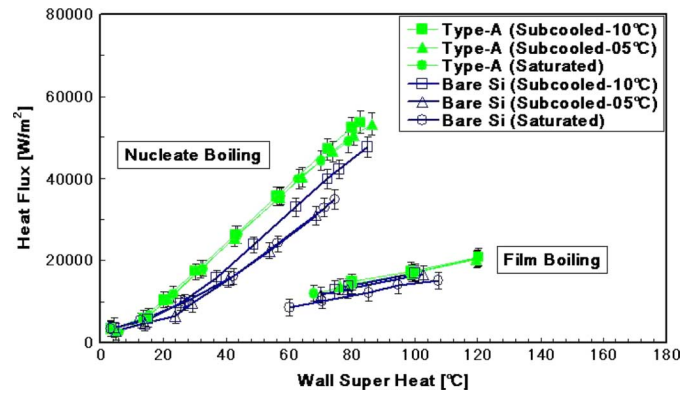


Fig. 3. Comparison of pool boiling curve for PF-5060 on MWCNTs, Type-A (9- μ m height) synthesized on silicon wafer with bare silicon wafer (saturation temperature of PF-5060 = 56 °C).

the pool boiling data for PF-5060 on Type-A MWCNTs under saturated and subcooled (5 °C and 10 °C) conditions. The wall heat flux values were found to increase as the liquid subcooling was increased. Also, the CHF point was obtained at higher wall super heat as the liquid subcooling was increased. Prior to obtaining the CHF condition for the 10 °C subcooling experiments, the chiller unit could not support the required cooling load. Hence, the data shown in Fig. 3 for subcooling of 10 °C is close to the CHF point. Under 5 °C subcooling, the CHF point was obtained at wall super heat of 86 °C and the associated heat flux was 5.3×10^4 W/m². This value is 72% higher than the corresponding CHF data for bare silicon wafer (control experiment), as shown in the figure. Type-A MWCNTs yields a modest enhancement in heat flux values than those for the bare silicon wafer. However, the CHF value for Type-A MWCNTs is only 10% higher than for bare silicon surface at a liquid subcooling of 10 °C.

For the film boiling regime, marginal enhancement in heat flux values was observed as the degree of subcooling was increased. The Leidenfrost point was achieved at higher wall super heat as the degree of subcooling increased. A similar trend was observed for the bare silicon wafer (as discussed in Section V). The heat flux level for Type-A MWCNT was slightly higher than or same (within the bounds of experimental uncertainty) compared to that for bare silicon wafer. Under 10 °C subcooled conditions, the heat flux values for Type-A MWCNTs was obtained to be 1.4×10^4 W/m² at 80 °C wall super heat. This is $\sim 6\%$ higher than that for bare silicon wafer (1.3×10^4 W/m² heat flux value) at the same wall super heat. As shown in Fig. 3, The Leidenfrost point for Type-A MWCNTs was observed at higher wall super heat for saturated and similar liquid subcooling conditions, compared to bare silicon wafer.

C. Experiments Using Type-B MWCNT Forests

Fig. 4 shows the results obtained from the experiments using Type-B MWCNT forests (25- μ m height). It was observed that Type-B MWCNTs yield similar boiling heat flux values (compared to Type-A) for a given wall super heat under saturated and subcooled nucleate boiling. At liquid subcooling of 10 °C the heat flux data at CHF was obtained as 6.7×10^4 W/m² at a wall super heat of 106 °C. Fig. 4 also compares the heat

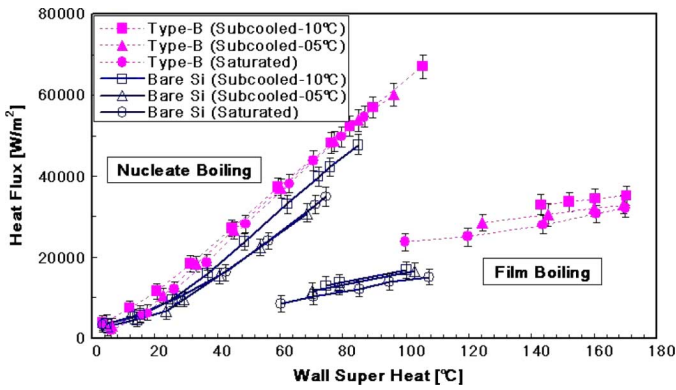


Fig. 4. Comparison of pool boiling curve for PF-5060 on MWCNTs, Type-B (25- μ m height) synthesized on silicon wafer with bare silicon wafer (saturation temperature of PF-5060 = 56 °C).

flux values for Type-B MWCNTs with those for bare silicon wafer. The CHF value for Type-B MWCNTs under 10 °C subcooling is 40% higher than bare silicon wafer and 25% higher than for Type-A MWCNT. Also, the heat flux value for Type-A and Type-B MWCNT is only 10% higher than bare silicon wafer at wall super heat of 85 °C and liquid subcooling of 10 °C.

For Type-B MWCNT, the extent of the wall superheat for transition boiling region (“boiling hysteresis”) was much longer and more distinct than Type-A MWCNT (and bare silicon wafer). During transition boiling, the portion of the heater surface under film boiling conditions was localized near outer the edge of the silicon wafer (near the clamps), and the portions of the heater surface under nucleate boiling conditions were localized near the center of the silicon wafer. After obtaining a steady-state wall super heat of 122 °C under saturated boiling conditions, a continuous vapor film was observed over the whole area of the exposed wafer. The vapor film was identifiable since it manifests as a shiny mirror type of surface which was observed clearly in the experiments.

For film boiling regime, at wall super heat of 160 °C, the heat flux values obtained for Type-B MWCNTs are 3.4×10^4 W/m², 3.2×10^4 W/m², and 3.1×10^4 W/m² under 10 °C subcooling, 5 °C subcooling, and saturated conditions, respectively. As the subcooling was increased, the Leidenfrost point was observed at higher wall super heat. This is consistent with similar observations for Type-A MWCNTs and bare silicon wafer. The Leidenfrost points for Type-B MWCNTs were obtained at wall superheat of 143 °C, 124 °C, and 100 °C under 10 °C subcooling, 5 °C subcooling, and saturated conditions, respectively. These wall superheat values are much higher than corresponding values obtained for the bare silicon wafer (Leidenfrost points were observed at 74 °C, 70 °C, and 60 °C wall super heat under 10 °C subcooling, 5 °C subcooling, and saturated conditions, respectively, for bare silicon wafer). The wall heat flux at the Leidenfrost point was 175% higher for Type-B MWCNTs than for bare silicon surface. The heat flux at the Leidenfrost point is more sensitive to subcooling for Type-B MWCNTs than for bare silicon or Type-A MWCNTs. The inherent morphology was found to be unaltered on inspection of the MWCNT structures before and after the experiments using SEM. This demonstrates that the bonding strength of the

MWCNT structures on the silicon wafer substrate is able to withstand the boiling experiments.

D. Comparison of Experiments

The heat flux values in nucleate boiling for both Type-A and Type-B MWCNTs are similar except at CHF. At CHF the wall heat flux values and the associated wall super heat under subcooled and saturated conditions are significantly different. The CHF values for Type-B MWCNTs are higher than those for Type-A MWCNTs. Type-B MWCNTs have 13% and 12% higher CHF values under 5 °C subcooled and saturated conditions, respectively, than Type-A MWCNT. It should be noted that these differences are within the bounds of the experimental error. However, a consistent trend is observed for the difference in performance between Type-A and Type-B MWCNTs close to the CHF. The associated wall super heat values for Type-B MWCNTs are around 10 °C higher than those for Type-A MWCNTs under both 5 °C subcooled and saturated conditions. In the nucleate boiling regime, as shown in Fig. 4, both Type-A and Type-B MWCNT forests enhanced wall heat flux for the different values of subcooling (10 °C, 5 °C, and 0 °C) compared to those for bare silicon wafer at a given wall super heat. For example, at 82 °C wall super heat and 10 °C liquid subcooling, Type-A and Type-B MWCNTs enhanced nucleate boiling heat flux by 23% and 19% compared to bare silicon wafer. The wall superheat and wall heat flux values under CHF conditions for Type-A and Type-B MWCNT forests are higher than those for bare silicon wafer for all of the saturated and subcooled experiments. At a wall superheat of 70 °C the nucleate pool boiling heat flux for Type-A and Type-B MWCNTs is $\sim 33\%$ higher than for bare silicon wafer at a subcooling of 5 °C.

The heat flux values for Type-B MWCNT are much higher than those for Type-A MWCNTs in film boiling. Under saturated condition, the heat flux values for Type-B is 2.2×10^4 W/m² at wall super heat of 120 °C which is 22% higher value than that for Type-A MWCNTs at the same wall super heat. It is observed that the heat flux is more sensitive to subcooling for film boiling on Type-B MWCNT than that for Type-A MWCNTs. For film boiling experiments at different subcooling (10 °C, 5 °C, and 0 °C), the heat flux values obtained for Type-B MWCNT are much higher than those for Type-A MWCNTs (and for the bare silicon wafer). Within the bounds of the experimental error, the heat flux values in the film boiling regime are almost identical for a given wall super heat for Type-A MWCNTs and for the bare silicon wafer. However, the Leidenfrost points for Type-A MWCNTs were observed to occur at a higher wall super heat for the same liquid subcooling. Hence, increasing the height of the MWCNT increases the super-heat required for obtaining the Leidenfrost point.

V. DISCUSSION

Table I shows the comparison of the maximum heat flux data (or CHF) obtained from this study with other experiments reported in the literature. The data of Mudawar and Anderson [4] was obtained on a machined copper surface—which has a much

TABLE I
MAXIMUM HEAT FLUX OR CHF VALUES—(W/cm²)

Surface Type	Saturated	10 °C Subcooling
Bare Silicon	3.5	4.8
Type-A MWCNT (9 microns height)	4.4	5.3
Type-B MWCNT (25 microns height)	4.5	6.7
Bare Silicon (Ujereh et al. [14])	11.4	-
MWCNT (~20-30 microns height, [14])	15.8	-
Porous surface (Chang and You [19])	29	-
Pin Fins (Honda et al. [8])	30	-
Porous (Hwang and Kavinay [21])	48	-
Porous (Liter and Kavinay [20])	76.2	-
Porous (Oktay [18])	84	-
Studs (Mudawar and Anderson [4])	105.4	-

higher nucleation site density due to pits and grooves on the surface [1]. The data by Honda *et al.* [8] was obtained at wall superheats at which the size of the pin fins are comparable in size to range of nucleating cavities (\sim order of 10 μm). The data by Oktay [18], Liter and Kavinay [20], Hwang and Kavinay [21] as well as Chang and You [19] were obtained for microporous and porous surfaces. These surfaces have a range of available cavity sizes that enhance nucleation site density. Consequently these experiments result in higher heat fluxes than for the MWCNT experiments (this study and Ujereh *et al.* [14]).

In the experiments using MWCNTs (this study and Ujereh *et al.* [14]) the MWCNT layers were synthesized on silicon wafers without any extraneous pits or grooves—hence, lower contribution to the total heat flux are expected from the reduction in nucleation site densities. The nucleation site densities can vary by wide margins for commercial surfaces (e.g., copper surfaces may have different size nucleating cavities depending on the machining or casting processes used during manufacture [1]).

From Table I it is observed that Ujereh *et al.* [8] obtained a heat flux of 11.4 W/cm² for saturated boiling of FC-72 on bare silicon compared to 3.5 W/cm² obtained in this study for saturated boiling of PF-5060. The size of the silicon chip used by Ujereh *et al.* [8] for boiling surface was 12.7 mm \times 12.7 mm. In contrast, the size of the boiling surface for the experiments reported in this study is 62 mm \times 32 mm (which is a 12 times bigger area). For the thermophysical property values of PF-5060 (and FC-72) the dominant Rayleigh–Taylor instability wavelength (and the dominant Taylor instability wavelength) that is believed to govern the CHF phenomena [1] is estimated to be \sim 6 mm. Since the lateral dimensions of the boiling surface used by Ujereh *et al.* [8] is of the same order as the dominant Taylor instability wavelength, the data reported is likely to be affected by edge effects (e.g., bubble nucleation on the edges of the heater and the “vapor jet” spacing [1] at CHF). The lateral dimensions of the boiling surface used in this study are \sim 5–10

times higher than the dominant Taylor instability wavelength. Therefore, the contributions from the edge effects are expected to be lower in this study. This explains the discrepancy observed in the heat fluxes for pool boiling on bare silicon wafer from the two studies.

Prior to synthesis of the MWCNTs, Ujereh *et al.* [14] performed surface modification of the silicon wafers by deposition of dendrimer-based catalysts which were subsequently calcined at high temperatures. Some degree of inherent surface roughness could be introduced on the silicon surface during the calcination process. This could help to enhance the nucleation site density on the boiling surface compared to the boiling surface used in this study, resulting in higher heat transfer for MWCNT. In this paper, an iron film of 5-nm thickness was deposited by electron beam evaporation to serve as a catalyst. Hence, the inherent surface roughness of the silicon wafer is expected to be less than 5 nm. The height of the MWCNT used by Ujereh *et al.* [14] was estimated to be 20–30 μm while the MWCNTs used in this study are of uniform height (9 μm and 25 μm).

Based on the experimental results, the potential mechanisms responsible for pool boiling heat transfer enhancement on heater surfaces coated with MWCNT are enumerated as follows.

- 1) “Nano-fin” effect: due to the enhanced axial thermal conductivity [13] and the enhanced surface area of the “hair like” protrusion of the MWCNT.
- 2) Quasi-periodic liquid-solid contacts that are believed to occur locally during pool boiling on a horizontal surface can be enhanced due to presence of the “hair like” protrusion of the MWCNT.
- 3) Disruption of the “microlayer” [1] in nucleate boiling and of the vapor-liquid vapor interface in film boiling.
- 4) Pinning of liquid-vapor contact line [22] on the nano-structures (MWCNT), leading to enhanced surface area underneath the nucleating and growing bubbles. This can potentially enhance heat transfer under individual bubbles

growing on MWCNT (compared to bubbles on the silicon surface).

Mudawar and Anderson [4] as well as Honda *et al.* [8] suggested that a possible reason for heat transfer enhancement on micro-structured surfaces was probably due to enhancement of the surface area (“pin-fins”). The pin fins were composed of the same material as the substrates. However, in this paper the silicon substrate has lower thermal conductivity than the axial thermal conductivity of individual MWCNTs [13]. Hence, the effect of the “hair-like” MWCNTs is not only in enhancing the surface area but also in enhancing the fin effectiveness (“*nano-fin*” effect). These “hair-like” MWCNT protrusions can also cause enhanced quasi-periodic liquid–solid contacts. This can cause enhanced local quenching of the heater surface. Such a dynamic mechanism may not exist (or may not be as dominant) on a plain atomically smooth silicon surface.

The results show (Figs. 3 and 4) low sensitivity of the heat transfer augmentation to the height of MWCNTs in the nucleate boiling regime. This is because in nucleate boiling, the size and distribution of the nucleation sites is expected to be the limiting variable than the height of the surface structures. It is postulated that in nucleate boiling the major proportion of heat flux occurs in a thin region under the nucleating bubbles called the “micro-layer” region [1] which is postulated to be of submicrometer thickness. The heights of the MWCNT in these experiments are greater than the size of the micro-layer. Therefore, both types of MWCNT are probably equally effective in disrupting the micro-layer causing enhanced evaporation. Hence, both types of MWCNTs result in similar heat flux enhancements for nucleate boiling at comparable wall superheat values. Alternately, it is also possible that the micro-layer region occupies a bigger area (and volume) provided by the lateral surface of the individual MWCNTs.

Increasing the height of the MWCNTs from 10 to 25 μm (and compared to a bare silicon wafer) increases the wall superheat required for CHF to occur. A potential mechanism for delaying the occurrence of CHF to higher superheats could be through enhanced formation of vapor stems under bubbles that trap superheated liquids at CHF (e.g., Gaertner [23]). This can occur due to enhanced heat transfer by the hair like protrusion of the MWCNTs into the superheated liquid layers trapped under the mushroom-shaped bubbles. Alternately, MWCNTs could also lead to formation of additional vapor stems due to presence of MWCNT on the surface due to reduction of the critical Rayleigh–Taylor instability wavelength. Such reduction in critical Rayleigh–Taylor instability wavelengths were also postulated for the observed increase in CHF for pool boiling on micro-porous surfaces [21]. It is possible that the reduction in instability wavelengths is more for Type-B MWCNTs than for Type-A MWCNTs—causing a higher value of CHF for Type-B MWCNTs. However, it should be noted that the conventional theories in boiling (e.g., instability theories) are based on continuum assumptions [1] that are applicable in the micro-scales. In the nano-scale regimes (e.g., on MWCNTs), the continuum assumptions may not be valid, and the transport mechanisms can be counter-intuitive to those based on continuum models. Additional investigations are therefore needed to conclusively verify the mechanisms responsible for extending the wall superheat

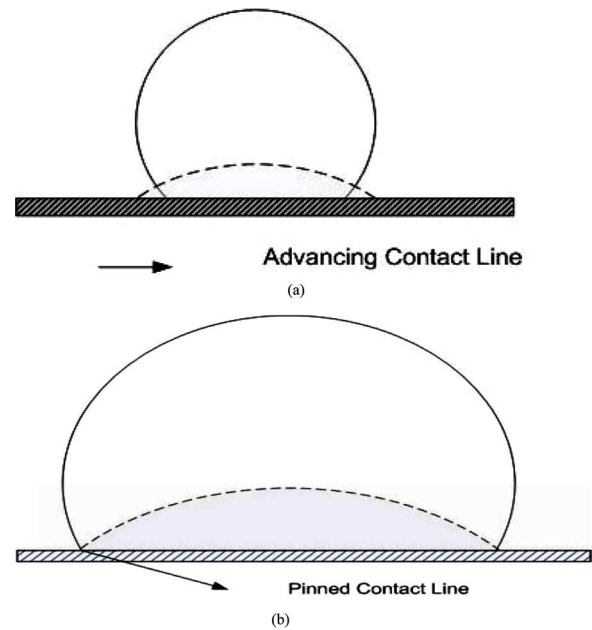


Fig. 5. Schematic depicting the different mechanisms for bubble growth during nucleate boiling for different surfaces. (a) On a smooth surface the advancing liquid–vapor contact line causes a smaller area under the bubble. (b) On a nano-structured surface, the contact line is “pinned” [18] causing the area under the bubble to be bigger than for a smooth surface. This can effectively enhance the rate of heat transfer for each bubble and also increase the bubble departure frequency.

required for CHF for boiling on nano-structured surfaces and to understand the effect of the height of the nano-structures on CHF.

Nano-structured surfaces are also postulated to cause pinning of the liquid–vapor contact line [22]. Such a peculiar behavior may lead to the formation of bigger bubbles during growth period in nucleate boiling (Fig. 5). Bigger bubbles during the growth period would lead to higher plan area under the bubbles and reduced growth period before bubble departure. These effects can result in enhanced evaporation rates and can augment the pool boiling heat transfer in nucleate boiling.

The experimental results for film boiling are consistent with numerical models reported in the literature. Previous numerical and experimental results by Banerjee and Dhir [24], [25] and Banerjee *et al.* [26] have shown that the dynamic value of the minimum vapor film thickness for film boiling of PF-5060 is approximately 10–15 μm . The authors had discussed that surface roughness (or for example artificially engineered surface micro/nano-structures) greater than 10 μm could disrupt the vapor films at the points of minimum vapor film thickness leading to possible collapse of film boiling.

Comparing the results of Type-A and Type-B MWCNT forests, it is observed that for Type-B (25- μm height) the film boiling is enhanced considerably than for Type-A (9- μm height). This shows that an MWCNT forest with heights greater than 10 μm possibly disrupts the vapor film (Fig. 6). Therefore, MWCNT forests with height greater than 10 μm have better efficacy in enhancing heat transfer in film boiling. The effect of subcooling on heat flux enhancement is therefore more pronounced for Type-B MWCNTs than for Type-A MWCNTs. Hence, in the film boiling regime (and at the Leidenfrost point)

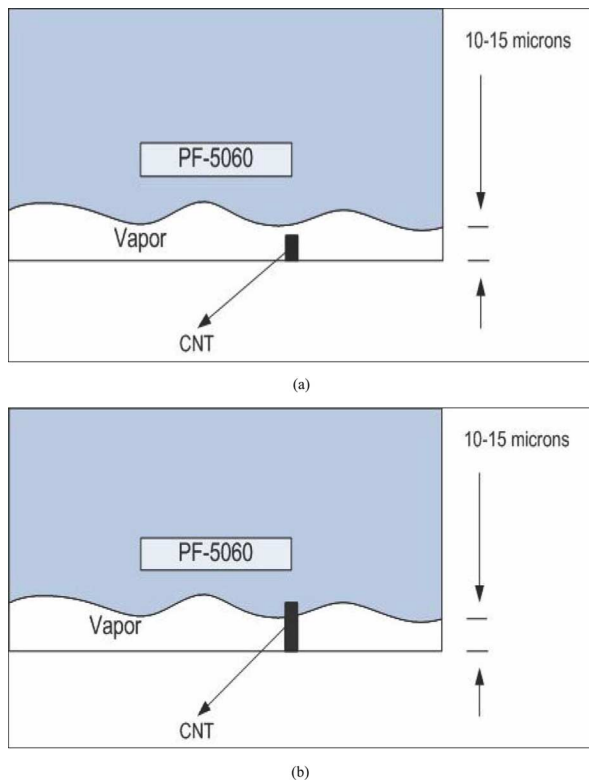


Fig. 6. Schematic depicting the hydrodynamic mechanisms during film boiling for the two types of MWCNTs. Only one MWCNT is shown for clarity. (a) The height of Type-A MWCNTs are $9\ \mu\text{m}$ which is less than the minimum vapor film thickness in film boiling (which is predicted by numerical models to be $10\text{--}15\ \mu\text{m}$) and therefore is not able to disrupt the vapor film. (b) The height of Type-B MWCNTs are $25\ \mu\text{m}$ which is more than the minimum vapor film thickness in film boiling and therefore it disrupts the vapor film.

the height of the MWCNT forests is critical to the efficacy of the heat transfer augmentation schemes.

VI. CONCLUSION

Boiling experiments were conducted with a bare silicon wafer and two silicon wafers each containing a uniform layer of vertically aligned MWCNTs of a different height (9 and $25\ \mu\text{m}$ height). The following insights were gathered from this study on the nature of the transport mechanisms on nano-structured surfaces:

- 1) In the nucleate boiling regime, the heat flux is found to be weakly sensitive to the height of the MWCNT.
- 2) For nucleate boiling, MWCNTs (both 9-- and $25\text{-}\mu\text{m}$ height) yield higher wall heat fluxes under $10\ ^\circ\text{C}$ subcooling, $5\ ^\circ\text{C}$ subcooling, and saturated conditions, compared to bare (smooth) silicon wafer.
- 3) Type-B MWCNTs were observed to augment CHF by 40% compared to bare silicon wafer under $10\ ^\circ\text{C}$ subcooling.
- 4) However, near CHF, the heat flux values for Type-B MWCNTs exceed those for Type-A MWCNTs by 25%.
- 5) In film boiling regime, the heat flux is strongly sensitive to the height of the MWCNT forests. For Type-B MWCNTs ($25\text{-}\mu\text{m}$ height) the heat flux was enhanced under $10\ ^\circ\text{C}$ subcooling, $5\ ^\circ\text{C}$ subcooling, and saturated conditions (compared to control experiments performed on bare silicon wafer). However, for Type-A MWCNTs ($9\text{-}\mu\text{m}$

height) the heat flux values are similar to that for the bare silicon wafer during film boiling. This is consistent with the dynamic models for film boiling reported in the literature.

- 6) During subcooled film boiling, Type-B MWCNTs are more sensitive to subcooling and causes greater enhancement of heat flux with increased subcooling (compared to bare silicon wafer and Type-A MWCNTs).
- 7) Based on the experimental data, the following transport mechanisms were identified to be the cause for the pool boiling heat flux enhancement on nano-structured surfaces:
 - a) enhanced heat transfer surface due to “nano-fins”;
 - b) enhanced liquid–solid contact and periodic quenching of the heater surface;
 - c) disruption of coupled thermal and hydrodynamic features (“micro-layer” in nucleate boiling and the vapor film at location of minimum thickness in film boiling);
 - d) “Pinning” of liquid–vapor contact line during nucleate boiling which alters the bubble nucleation and growth profile as well as the bubble departure frequency.

ACKNOWLEDGMENT

The authors would like to thank Dr. M. Zhang, Dr. S. Feng, and Dr. R. Baughman at the Nanotech Institute, University of Texas at Dallas, for their help with synthesizing the MWCNTs on silicon wafers.

REFERENCES

- [1] S. G. Kandlikar, M. Shoji, and V. K. Dhir, *Handbook of Phase Change: Boiling and Condensation*. Philadelphia, PA: Taylor and Francis, 1999.
- [2] C. Ramaswamy, Y. K. Joshi, W. Nakayama, and W. B. Johnson, “Combined effects of subcooling and operating pressure on the performance of a two-chamber thermo-siphon,” *IEEE Trans. Compon. Packag. Technol.*, vol. 23, no. 1, pp. 61–69, Mar. 2000.
- [3] C. Ramaswamy, Y. Joshi, W. Nakayama, and W. B. Johnson, “Effects of varying geometrical parameters on boiling from microfabricated enhanced structures,” *ASME J. Heat Transfer*, vol. 125, pp. 103–109, 2003.
- [4] I. Mudawar and T. M. Anderson, “Optimization of enhanced surfaces for high flux chip cooling by pool boiling,” *Trans. ASME J. Electron. Packag.*, vol. 115, pp. 89–100, 1993.
- [5] J. Coursey, J. K. H. Roh, J. Kim, J. H. , and P. J. Boudreaux, “Graphite foam thermosiphon evaporator performance: Parametric investigation of the effects of working fluid, liquid level, and chamber pressure,” presented at the Proc. IMECE2002, New Orleans, LA, 2002, unpublished.
- [6] B. Gebhart and N. Wright, “Boiling enhancement on microconfigured-surfaces,” *Int. Commun. Heat and Mass Transfer*, vol. 15, pp. 141–149, 1988.
- [7] W. J. Miller, B. Gebhart, and N. T. Wright, “Effects of boiling history on a microconfigures surface in a dielectric liquid,” *Int. Commun. Heat and Mass Transfer*, vol. 17, pp. 389–398, 1990.
- [8] H. Honda, H. Takamastu, and J. J. Wei, “Enhanced boiling of FC-72 on silicon chips with micro-pin fins and sub-micron scale roughness,” *ASME J. Heat Transfer*, pp. 383–390, 2002.
- [9] M. Bahrami, M. M. Yovanovich, and J. R. Culham, “Role of random roughness on thermal performance of micro-fins,” in *Proc. Heat Transfer Conf.*, San Francisco, CA, Jul. 17–22, 2005, Paper No. HT2005-72712.
- [10] R. Furberg, “Enhanced boiling heat transfer from a novel nanodendritic micro-porous copper structure,” Ph.D. dissertation, KTH Royal Inst. Technol., Stockholm, Sweden, 2006.
- [11] S. Iijima, “Helical microtubules of graphitic carbon,” *Nature* 354, pp. 56–58, 1991.

- [12] S. Berber, Y. K. Kwon, and D. Tomanek, "Unusually high thermal conductivity of carbon nanotubes," *Phys. Rev. Lett.*, vol. 84, pp. 4613–4616, 2000.
- [13] P. Kim, L. Shi, A. Majumdar, and P. L. McEuen, "Thermal transport measurements of individual multiwalled nanotubes," *Phys. Rev. Lett.*, vol. 87, no. 21, pp. 215502:1–215502:4, Nov. 19, 2001.
- [14] O. S. Ujereh, I. Mudawar, P. B. Amama, T. S. Fisher, and W. Ou, "Enhanced pool boiling using carbon nanotube arrays on a silicon surface," in *Proc. ASME-IMECE 2005*, Orlando, FL, Nov. 5–11, 2005, 2005, Paper No. IMECE2005-80065.
- [15] H. S. Ahn, N. Sinha, M. Zhang, D. Banerjee, S. Feng, and R. Baughman, "Pool boiling experiments on multiwalled carbon nanotube (MWCNT) forests," *J. Heat Transfer*, vol. 128, pp. 1335–1342, Dec. 2006.
- [16] M. Zhang, S. Fang, A. A. Zakhidov, S. B. Lee, A. E. Aliev, C. D. Williams, K. R. Atkinson, and R. Baughman, "Strong, transparent, multifunctional, carbon nanotube sheets," *Science*, vol. 309, pp. 1215–1219, 2005.
- [17] H.-S. Ahn, N. Sinha, and D. Banerjee, "Micromachined temperature sensor arrays for studying micro-scale features in film boiling," in *Proc. ASME-IMECE 2005*, Orlando, FL, Nov. 5–11, 2005, Paper No. IMECE2005-81869.
- [18] S. Oktay, "Departure from natural convection (DNC) in low temperature boiling heat transfer encountered in cooling micro-electronic LSI devices," in *Heat Transfer 1982, Proc. 7th Int. Heat Transfer Conf.*, Munich, Germany, 1982, vol. 4, pp. 113–118.
- [19] J. Y. Chang and S. M. You, "Boiling heat transfer phenomena from micro-porous and porous surfaces in saturated FC-72," *Int. J. Heat and Mass Transfer*, vol. 40, no. 18, pp. 4437–4447, 1997.
- [20] S. G. Lister and M. Kavinay, "Pool-boiling CHF enhancement by modulated porous-layer coating: Theory and experiment," *Int. J. Heat and Mass Transfer*, vol. 44, pp. 4287–4311, 2001.
- [21] G. S. Hwang and M. Kavinay, "Critical heat flux in thin, uniform particle coatings," *Int. J. Heat and Mass Transfer*, vol. 49, pp. 844–849, 2006.
- [22] K. Sefiane, "On the role of structural disjoining pressure and contact line pinning in critical heat flux enhancement during boiling of nanofluids," *Appl. Phys. Lett.*, vol. 89, pp. 044106-1–044106-3, 2006.
- [23] R. F. Gaertner, "Distribution of active sites in the nucleate boiling of liquids," in *Proc. Chem. Eng. Progress Symp. Ser.*, 1963, vol. 59, pp. 52–61.
- [24] D. Banerjee and V. K. Dhir, "Study of subcooled film boiling on a horizontal disc: Part 1 analysis," *J. Heat Transfer*, vol. 123, pp. 271–284, 2001.
- [25] D. Banerjee and V. K. Dhir, "Study of subcooled film boiling on a horizontal disc: Part 2 experiments," *J. Heat Transfer*, vol. 123, pp. 285–293, 2001.
- [26] D. Banerjee, G. Son, and V. K. Dhir, "Conjugate thermal and hydrodynamic analysis of saturated film boiling from a horizontal surface," *ASME HTD Part 3*, vol. 334, pp. 57–64, 1996.



Hee Seok Ahn was born in Seoul, Korea, in 1965. He received the B.S. and M.S. degrees in mechanical engineering from Korea University, Seoul, Korea, in 1988 and 1990, respectively, and the Ph.D. degree in mechanical engineering from Texas A&M University, College Station in 2007.

From 1996 to 2002, he held a position as a Senior Research Engineer with Hyundai Motor Company, Korea. His research interests include micro-scale heat transfer in boiling, convective heat and mass transfer, electronic cooling, turbine and automotive

engine cooling, micro fabrication, and CFD.



Vijaykumar Sathyamurthi received the B.E. degree in mechanical engineering (with honors) from Nagpur University, Nagpur, India, in 2003 and the M.S. degree in mechanical engineering from Texas A&M University, College Station, in 2006. He is currently pursuing the Ph.D. degree in mechanical engineering at Texas A&M University.

He is a Graduate Assistant Researcher in the Multiphase flow and Heat Transfer Laboratory at Texas A&M University. His research interests include, boiling heat transfer, computational fluid

dynamics and dynamical systems.

Mr. Sathyamurthi is a student member of ASME and IMAPS.



Debjyoti Banerjee received the B.S. degree (with honors) in mechanical engineering from the Indian Institute of Technology (IIT), Kharagpur, and the M.S. and Ph.D. degrees in mechanical engineering (with minor in MEMS) from the University of California, Los Angeles (UCLA).

He was a Manager of Advanced Research and Technology at Applied Biosystems, Inc. (ABI). At ABI, he managed the Fluidics and Device Engineering Group for microfluidics product development. He has been awarded one patent on

microfluidics and nanotechnology. He has submitted one provisional patent, five patent applications, and more than 25 invention disclosures while working at Coventor, Inc., NanoInk, Inc., and at ABI. Previously at NanoInk, Inc., he was instrumental in developing from concept to a commercial product (called "InkWells"). InkWells are microfluidics platforms used for bio/nano-technology applications. From January 2005, he has been an Assistant Professor of Mechanical Engineering, Texas A&M University, College Station, and supervising student research activities at the Multi Phase Flow and Heat Transfer Laboratory. His research interests include: multiphase flows (boiling), MEMS/microfluidics and bio/nano-technologies (carbon nanotubes, dip pen nanolithography).

Dr. Banerjee is a member of the AIAA, ASEE, ASME, and SAE. He received invitational membership to four honor societies: Tau Beta Pi (Engineering), Sigma Xi (Scientific Research), Phi Kappa Phi (Academic Excellence), and Gamma Beta Phi (Social Service). He received the Best Journal Paper Award (2002) from the ASME Heat Transfer Division for a paper in the ASME Journal of Heat Transfer. He received the Best Mechanical Engineering Student Award (Endowment, 1992) at IIT graduation convocation and the J. C. Bose National Science Talent Scholarship (Book Grant, 1988) from the Government of India. He received the New Investigator Award (2005) from the Texas Space Grants Consortium (TSGC), AFRL Summer Faculty Fellowship (2006) from ASEE, and the Morris Foster Faculty Fellowship (2007–2009) from Mechanical Engineering Department, Texas A&M University.